Conditional Controllable Image Fusion

Bing Cao[1,2] **Xingxin Xu**[3] **Pengfei Zhu**[1]* **Qilong Wang**[1] **Qinghua Hu**[1]

[1]College of Intelligence and Computing, Tianjin University, Tianjin, China
[2]State Key Laboratory of Integrated Services Networks, Xidian University, Xi'an, China
[3]School of New Media and Communication, Tianjin University, Tianjin, China
`{caobing, xuxingxin, zhupengfei, qlwang, huqinghua}@tju.edu.cn`

Abstract

Image fusion aims to integrate complementary information from multiple input images acquired through various sources to synthesize a new fused image. Existing methods usually employ distinct constraint designs tailored to specific scenes, forming fixed fusion paradigms. However, this data-driven fusion approach is challenging to deploy in varying scenarios, especially in rapidly changing environments. To address this issue, we propose a conditional controllable fusion (CCF) framework for general image fusion tasks without specific training. Due to the dynamic differences of different samples, our CCF employs specific fusion constraints for each individual in practice. Given the powerful generative capabilities of the denoising diffusion model, we first inject the specific constraints into the pre-trained DDPM as adaptive fusion conditions. The appropriate conditions are dynamically selected to ensure the fusion process remains responsive to the specific requirements in each reverse diffusion stage. Thus, CCF enables conditionally calibrating the fused images step by step. Extensive experiments validate our effectiveness in general fusion tasks across diverse scenarios against the competing methods without additional training. The code is publicly available.[†]

1   Introduction

Image fusion aims at integrating complementary information from multi-source images, fusing a new composite image containing richer details [1]. It has been applied in various scenarios that single image contains incomplete information, such as multi-modal fusion (MMF) [2, 3], multi-exposure fusion (MEF) [4, 5], multi-focus fusion (MFF) [6], and remote sensing fusion [2]. The fused image inherits the strengths of both modalities, resulting in a composite with enhanced visual effects [7]. These fusion tasks have diverse downstream applications in computer vision, including object detection [8–10], semantic segmentation [11, 12], and medical diagnosis [13] because the comprehensive representation of images with multi-scene information contributes to the improved performance of applications.

Recently, numerous image fusion methods [14–17] have been proposed, such as traditional fusion methods [18], CNN-based fusion methods [19, 20] and GAN-based methods [21]. While these methods produce acceptable fused images in certain scenarios, they are also accompanied by significant drawbacks and limitations: (i) They are often tailored for specific scenarios or individual tasks, limiting their adaptability across diverse applications; (ii) These methods necessitate training and consume substantial computational resources, posing limitations in terms of time and resource requirements. Lately, denoising diffusion probabilistic models (DDPM) have emerged as an iterative

---

*Corresponding author.
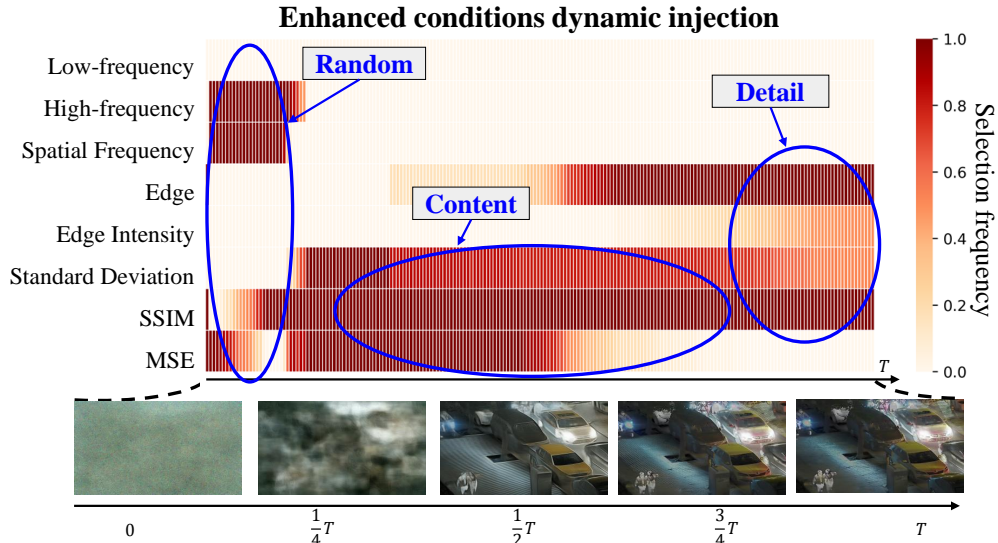[†]`https://github.com/jehovahxu/CCF`

Figure 1: The conditions selection statistics during the sampling process of the LLVIP dataset. The distinct process of sampling has different favor of the conditions. The crucial role that diverse conditions play in controlling various image generation processes. Throughout the diffusion sampling, different conditions are dynamically selected to best suit the generation requirement at each stage.

generation framework, showcasing impressive capabilities in unconditional generation. Inspiringly, numerous researchers explored its controllable aspects. ILVR [22] proposed iterative latent variable refinement with a reference image to control image translation. Some recent works [23, 24] employed the diffusion model for image fusion, which fuses images in fixed fusion paradigms (fixed fusion conditions) by using its inherent reconstruction capacity. However, these approaches are not qualified for sample-customized fusion with dynamic conditions. At present, general image fusion with controllable diffusion models is still a challenging problem, warranting further exploration.

In this paper, we propose a diffusion-based controllable conditional image fusion (CCF) framework, which controls the fusion process by adaptively selecting optimization conditions. We construct a condition bank of generally used conditions, categorizing them into *basic*, *enhanced*, and *task-specific* conditions. CCF dynamically assigns fusion conditions from the condition bank and continuously injects them into the sampling process of diffusion. To enable flexible integrated conditions, we further propose a sampling-adaptive condition selection (SCS) mechanism that tailors condition selection at different denoising steps. The iterative refinements of the sampling are based on the pre-trained diffusion model without additional training. It is worth noting that the estimated fused images are conditionally controllable during the iterative denoising process. The diffusion process seamlessly integrates these conditions during the sampling process, decreasing potential impacts. As illustrated in Fig. 1, the generation process emphasizes different aspects at various sampling steps. In the initial stages, the condition selection is influenced by random noise, resulting in a random selection. During the intermediate stages, there is a shift towards content components. In the final stage, the emphasis moves to generating and selecting texture details. These various conditional factors contribute to different aspects of fusion results and demonstrate the necessity and effectiveness of introducing specific conditions in different stages. To the best of our knowledge, we for the first time propose a conditional controllable framework for image fusion. The main contributions are summarized as follows:

- We propose a pioneering conditional controllable image fusion (CCF) framework with a condition bank, achieving controllability in various image fusion scenarios and facilitating the capability of dynamic controllable image fusion.

- We propose a sampling-adaptive condition selection mechanism to subtly integrate the condition bank into denoising steps, allowing adaptive condition selection on the fly without additional training and ensuring the dynamic adaptability of the fusion process.

- Extensive experiments on various fusion tasks have confirmed our superior fusion performance against the competing methods. Furthermore, our approach qualifies for interactive manipulation of the fusion results, demonstrating our applicability and efficacy.

2

2 Related Work

Image fusion focuses on producing a unified image that amalgamates complementary information sourced from multiple source images [25].

Specialized. Focus on specialized tasks such as VIF, several early approaches [26–28] relied on CNNs to address challenges across various scenarios. GTF [29] defined the objective of image fusion as preserving both intensity information in infrared images and gradient information in visible images. Besides that, researchers started artificially incorporating prior knowledge to aid in the fusion process. CDDFuse [30] introduced the concept of high and low-frequency decomposition with dual-branch as prior information. Diverging from approaches tailored to single scenarios, numerous methods are now exploring the development of a unified fusion framework.DDFM [24] represents the pioneering training-free method that employs a diffusion model for multi-modal image fusion.

Generalized. Not limited to specialized applications, researchers aim to extend its use to generalized tasks. U2Fusion [31] introduced a unified framework capable of adaptively preserving information and facilitating joint training across various task scenarios. Additionally, SwinFusion [32] proposed a cross-domain distance learning method that has been extended to form a unified framework encompassing diverse task scenarios. Defusion [33] employs self-supervised learning techniques to decompose images and subsequently adaptively fuse them. TC-MoA [34] proposed a novel task-customized mixture of adapters for generating image fusion with a unified model, enabling adaptive prompting for various fusion tasks.

Nevertheless, these methods cannot control image fusion for adaptation to different scenarios. Therefore, we propose a method that enables image control, manipulating the fused image through existing conditions on our condition bank.

3 Preliminary

Denosing diffusion probabilistic models (DDPM) is a class of likelihood-based models that shows remarkable performance [35] with a stable training objective in unconditional image generation. The diffusion process entails incrementally introducing Gaussian noise to the data until it reaches a state of random noise. For a clean sample $x_0 \sim q(x_0)$ each step within the diffusion process constitutes a Markov Chain, encompassing a total of T steps, relying on the data derived from the preceding step. Gaussian noise is added as follows:

$$q(x_t|x_{t-1}) = \mathcal{N}(x_t; \sqrt{1-\beta_t}x_{t-1}, \beta_t I), \tag{1}$$

where $\{\beta_t\}_{t=1}^T$ is the variance schedule of each diffusion step which is fixed and predefined. The generative process learns the inverse of the DDPM forward (diffusion) process, sampling from a distribution by reversing a gradual denoising process. We can directly sample x_t at any t step based on the original data $x_t \sim q(x_t|x_0)$ and via the reparameterization, it can be redefined:

$$x_t = \sqrt{\bar{\alpha}_t}x_0 + \sqrt{1-\bar{\alpha}_t}\epsilon, \tag{2}$$

where defined $\alpha_t := 1 - \beta_t$ and $\bar{\alpha} := \prod_{i=1}^t \alpha_i$. The diffusion process introduces noise to the data, whereas the inverse process represents a denoising procedure called sampling. In particular, stats with a noise $x_T \sim \mathcal{N}(0, I)$, the diffusion model learns to produce slightly less-noisy sample x_{T-1}, the process can be formulate by:

$$p_\theta(x_{t-1}|x_t) = \mathcal{N}(x_{t-1}; \mu_\theta(x_t, t), \Sigma_\theta(x_t, t)). \tag{3}$$

Utilizing the properties of Markov chains, decomposing μ_θ and Σ_θ, the process of generation is expressed as:

$$x_{t-1} = \frac{1}{\sqrt{\alpha_t}}(x_t - \frac{1-\alpha_t}{\sqrt{1-\bar{\alpha}_t}}\epsilon_\theta(x_t, t)) + \sigma_\theta^2(t)I, \tag{4}$$

where, $\sigma_\theta^2(t) = \Sigma_\theta(t) = \frac{(1-\alpha_t)(1-\bar{\alpha}_{t-1})}{1-\bar{\alpha}_t}$, ϵ_θ signifies the output of a neural network, commonly a U-Net. This neural network predicts the noise ϵ_θ at each step, which is utilized for the denoising procedure. It can be observed that variance is a fixed quantity, because of diffusion process parameters being constant, whereas the mean is a function dependent on x_0 and x_t. However, the stochastic process poses challenges in controlling the generative process.
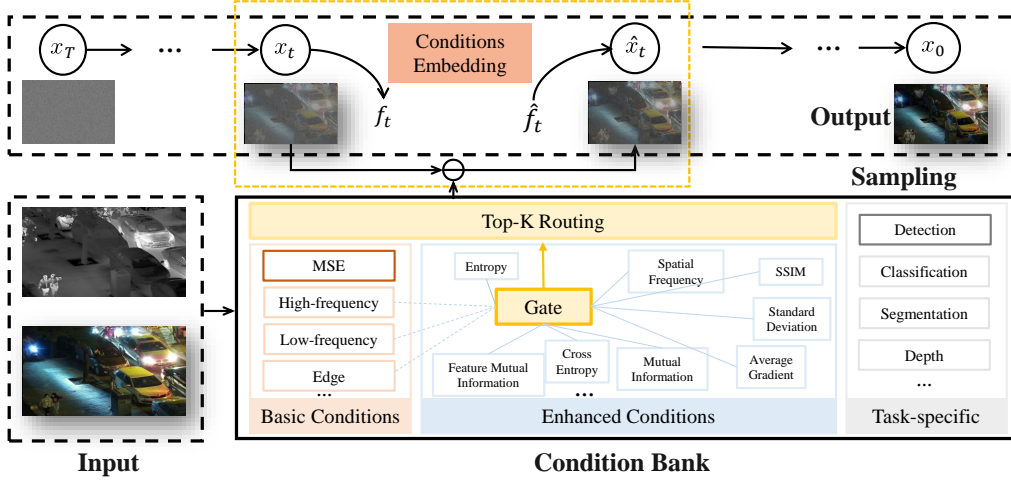
Figure 2: Illustrates the pipeline of the proposed CCF. The framework comprises two components: a sampling process utilizing a pre-trained DDPM and a condition bank with SCS.

4 Method

Leveraging the reconstruction capability of unconditional DDPM, we introduced a new controllable conditional image fusion (CCF) framework. Our approach accomplishes dynamically controllable image fusion via progressive condition embedding. In particular, we introduced a condition bank that regulates the incorporation of fusion information using conditions. It allows for combining the dynamic selection of multiple conditions to achieve sampling-adaptive fusion effects. As shown in Fig. 2, we illustrate our CCF framework in detail with visible-infrared image fusion (VIF). The goal is to generate a fused image $f \in \mathcal{R}^{H \times W \times N}$ from visible $v \in \mathcal{R}^{H \times W \times N}$ and infrared $i \in \mathcal{R}^{H \times W \times N}$ images, where H, W and N denote height, width, and channel numbers, respectively.

4.1 Controllable Conditions

Firstly, we provide the notation for the model formulation. For each sampling instance, a pre-trained DDPM represents unconditional transition $p_\theta(x_{t-1}|x_t)$. Our method facilitates the inclusion of conditional c during the sampling step of unconditional transformation, without no additional training. For this purpose, we sample images from the conditional distribution $p(x_0|c)$ given condition c:

$$p_\theta(x_0|c) = \int dx^{(1:T)} p_\theta(x^{(0:T)}|c),$$

$$p_\theta(x^{(0:T)}|c) = p(x_T) \prod_{t=1}^{T} p_\theta(x_{t-1}|x_t, c). \tag{5}$$

Each transition $p_\theta(x_{t-1}|x_t, c)$ of the generative process depends on the condition c. From the property of the forward process that latent variable x_t can be sampled from x_0 in closed-form, denoised data x_0 can be approximated with model prediction $\epsilon_\theta(x_t, t)$:

$$x_{0|t} \approx f_\theta(x_t, t) = \frac{(x_t - \sqrt{1 - \bar{\alpha}_t} \epsilon_\theta(x_t, t))}{\sqrt{\bar{\alpha}_t}}. \tag{6}$$

To compute $p(x_t|c)$, we can derive it from the Stochastic Differential Equation (SDE) [36]. For brevity, $x_{0|t}$ is abbreviated as x_0, and the expression is given by:

$$\nabla_{x_t} \log p(x_t) = -\frac{x_t - \sqrt{\bar{\alpha}_t} x_0}{1 - \bar{\alpha}_t}. \tag{7}$$

Classifier Guidance [37] can be intuitively elucidated via the score function, which logarithmically decomposes the conditional generation probability using Bayes' theorem:

$$\nabla \log p(x_t|c) = \nabla \log p(x_t) + \nabla \log p(c|x_t). \tag{8}$$
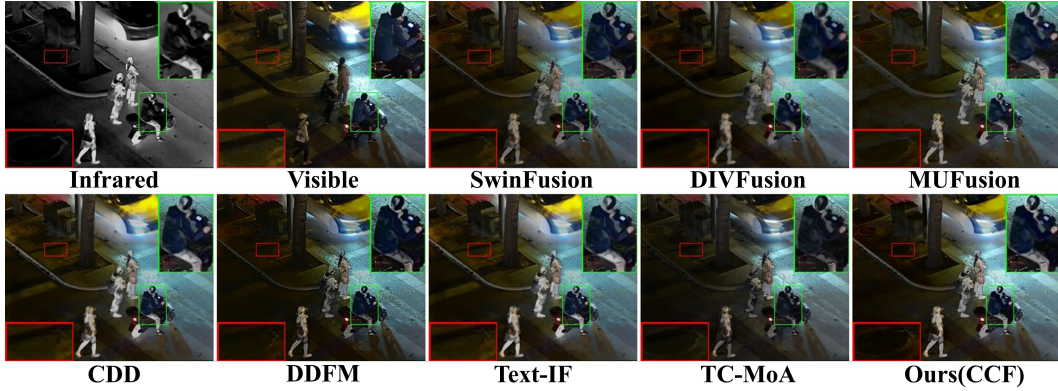
4

Figure 3: Qualitative comparisons of our CCF and the competing methods on VIF fusion task of LLVIP dataset.

Diffusion posterior sampling can yield a more favorable generative trajectory, especially in noisy settings, [38] estimation $\log p(c|x_t)$ as follows:

$$\nabla \log p(c|x_t) \approx \nabla \log p(c|\hat{x}_0). \tag{9}$$

Further, as demonstrated in [39], we can express the score function as:

$$\nabla \log p(c|x_t) \approx \nabla \log p(c|\hat{x}_0) = f_\theta(x_t, t) - \lambda \nabla ||C - \mathcal{A}(x_0)||_2. \tag{10}$$

Here, $\mathcal{A}(\cdot)$ can be linear or nonlinear operation. We represent $||C - \mathcal{A}(x_0)||$ as δ_C. Now, the objective is to obtain $\hat{x}_0$ and incorporate the condition into it. We can minimize δ_C to regulate the sampling within the diffusion process. In the following section, we will provide a detailed explanation of how to build a condition bank and how to select conditions.

4.2 Condition Bank

We empirically construct a *condition bank* and divide the image constraints into three categories: basic fusion conditions, enhanced fusion conditions, and task-specific fusion conditions. Basic fusion conditions are utilized throughout the entire sampling process, while enhanced fusion conditions are dynamically selected. Task-specific fusion conditions are manually optional, tailored to specific tasks, and may possess unique attributes that can be customized for various task scenarios. All conditions can be part of the enhanced condition set, enabling dynamic selection. The condition bank presented in this paper includes some common conditions, but additional conditions can be explored and utilized in other scenarios.

In the above formulation, each conditional Markov transition with the given condition c is shown in Eq. 5. In particular, we constructed a condition bank that allows us to select required conditions $C = \{c_1, c_2, ..., c_n\}$, subsequently integrating them into the unconditional DDPM for executing conditional image fusion. Let C represent a condition bank comprising a series of conditions. The function δ_C represents the difference between the source images with the given condition. In every sampling step t, the difference function δ_{c_i} can be minimized using gradient descent. These conditions help regulate the image information within each modality involved in the fusion process.

Basic Conditions. As shown in Fig. 2, basic conditions are essential to select for a basic generation. The basic conditions aim to synthesize a foundational fused image, offering an initial, coarse representation. The fused image serves as a primary fusion output, capturing essential features from the source images, though it may suffer from detail loss or texture blur. Notably, different scenarios may require adjustments to the basic condition, as the specific requirements of each fusion task, such as clarity, contrast, and other priorities, can influence its selection. Tailoring the basic condition to align with the unique demands of each task thus ensures an effective fusion process.

Enhanced Conditions. Besides basic conditions, we added enhancement conditions for refining the image generation process. The condition bank contains a variety of enhanced conditions, inspired by various Image Quality Assessments (IQA) such as SSIM, and standard deviation(SD). These conditions can be integrated into the CCF generation process to improve the quality of the generated images. The enhanced conditions can be selected with SCS algorithm, allowing different steps of the diffusion sampling process to be optimized with different conditions. This targeted approach ensures

that each phase of the image generation is adapted to the specific requirements of that stage, resulting in higher quality fused images.

Task-specific Conditions. The purpose of image fusion is to facilitate various downstream tasks. To meet the specific requirements of these tasks, we offer task-specific conditions. These conditions can be manually added to ensure that the fusion process is tailored to suit the downstream applications better. For example, a detection condition can be introduced by utilizing the feature extracted by a detection network $F = D(x)$. The detection condition is formulated as $||F(x), F(M)||_2$, where $X \in \{x_0\}_i^m$ and M is the set of m modalities. Other task-specific conditions can be similarly tailored to optimize the fusion process for different tasks. By integrating these task-specific conditions, the image fusion process can be precisely aligned with the demands of various applications, enhancing the effectiveness and utility of the generated images.

4.3 Sampling-adaptive Condition Selection

During the diffusion sampling process, it is crucial to focus on generating distinct aspects of the image. To address this, we designed an algorithm that dynamically selects the appropriate condition from the condition bank to fit each sampling stage. This selection process can be denoted as $C_{opt} = \text{Top}_k\{\text{Gate}(C)\}$. The C_{opt} is the selected condition, and Gate is the gate of selection. We hypothesize that rapidly changing conditions during the sampling process should be prioritized as they indicate greater significance at that generation stage. Inspired by multi-task learning [40], the gate of conditions can be calculated using the following formula:

$$\text{Gate} = [\omega_1, ..\omega_c], \omega_i(t) = \omega_i(t-1) - \bigtriangledown\omega_i. \tag{11}$$

The $\omega_i(t-1)$ represents the condition gradient from the previous step, and the $\bigtriangledown\omega_i$ is calculated as:

$$\bigtriangledown\omega_i = \sum_i |G_W^i(t) - \mathbb{E}[G_W^i(t)] \times \alpha_i(t)|_1, \tag{12}$$

where, $G_W = ||\omega_i(t)L_i(t)||_2$, $L_i(t)$ represents the condition gradient at step t, and the value can be calculated using a gradient descent algorithm in minimize δ_{c_i}. The $\alpha_i(t)$ is defined as:

$$\alpha_i(t) = [\frac{\widetilde{L_i}}{\mathbb{E}[\widetilde{L_i}]}]^\theta, \tag{13}$$

where, $\widetilde{L_i} = \frac{L_i(t)}{L_i(t-1)}$, θ is a hyper-parameter. By incorporating this SCS algorithm, we can efficiently choose the most relevant condition for each step in the diffusion process, thereby enhancing the quality of the conditional image fusion.

5 Experiments

Datasets. We conduct experiments in three image fusion scenarios: multi-modal, multi-focus, and multi-exposure image fusion. For multi-modal image fusion task, we conducted experiments on the LLVIP [41] dataset and referred to the test set outlined in Zhu et al. [34]. For MEF and MFF, our testing procedure followed the test setting in MFFW dataset [42] and MEFB dataset [43], respectively. Additionally, we test our method on the TNO dataset and Harvard medical dataset to assess our method's performance within the multi-modal fusion domain, detailed in App. B and H.

Implementation Details. Our method utilizes a pre-trained diffusion model as our foundational model [44]. This model was directly applied without any subsequent fine-tuning for specific task requirements during our experiments. The experiments are conducted on Huawei Atlas 800 Training Server with CANN and NVIDIA RTX 3090 GPU. Experimental settings are shown in App. A.

Evaluation Metrics. We evaluated the fusion results in both quantitative and qualitative. Qualitative evaluation primarily hinges on subjective visual assessments conducted by individuals. We expect that the fused image will exhibit rich texture details and abundant color saturability. Objective evaluation primarily focuses on measuring the quality assessments of individual fused images and their deviations from the source images. For different task scenarios, the different evaluation metrics used, specifically, we employ six metrics including Structural Similarity (SSIM), Mean squared error (MSE), correlation coefficient (CC), peak signal-to-noise ratio (PSNR), modified fusion artifacts measure (Nabf). In the MFF and MEF tasks, considering the different task scenarios, we employ standard deviation (SD), average gradient (AG), spatial frequency (SF), and sum of the correlations of differences (SCD) for evaluation metrics.
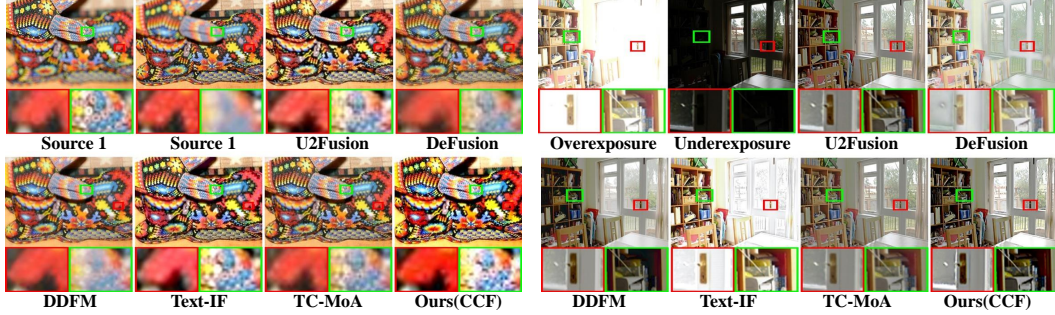
Figure 4: Qualitative comparisons of various methods in MFF task from MFFW dataset.

5.1 Evaluation on Multi-Modal Image Fusion

For multi-modal image fusion, we compare our method with the state-of-the-art methods: Swin-Fusion [32], DIVFusion [45], MUFusion [46], CDDFuse [30], DDFM [24], Text-IF [47], and TC-MoA [34] and on the LLVIP dataset. More datasets and comparison methods are shown in App. B. Note that our method, like DDFM, does not require additional tuning.

Quantitative Comparisons. We employ five quantitative metrics to evaluate our model, as shown in Table 1. Our method demonstrated exceptional performance across various evaluation metrics. On the LLVIP dataset, our method achieved the best results in SSIM, MSE, and CC indicators. Specifically, our method outperformed others in SSIM and CC, with improvements of 0.02 and 0.035 over the second-best results, respectively. Additionally, lower MSE values indi-

Table 1: Comparison with SOTAs in the LLVIP dataset. The red/blue/green indicates the best, runner-up and third best.

	SSIM↑	MSE↓	CC↑	PSNR↑	Nabf↓
	LLVIP Dataset				
SwinFusion [32]	0.81	2845	0.668	32.33	0.023
DIVFusion [45]	0.82	6450	0.655	21.60	0.044
MUFusion [46]	1.10	2069	0.648	31.64	0.030
CDDFuse [30]	1.18	2545	0.670	32.13	0.016
DDFM [24]	1.18	2056	0.668	36.10	0.004
Text-IF [47]	1.20	2135	0.669	31.97	0.023
TC-MoA [34]	1.20	2790	0.666	33.00	0.017
CCF (ours)	1.22	1694	0.705	32.71	0.005

cate better performance, with our method showing a reduction of 362 compared to the second-best methods in these metrics. This indicates that our method retains more information from the source images. The results show suboptimal performance in Nabf but are close to the best values, indicating the fused image with less noise. Notably, our method does not necessitate turning and holds its ground against methods requiring training. Compared to existing LLM tuning methods, our model performs slightly worse in terms of PSNR. This demonstrates the excellent performance of our model, achieving high performance across almost all indicators in a tuning-free model.

Qualitative Comparisons. Furthermore, the incorporation of the basic condition and enhanced conditions enables effective preservation of the background and texture. This comparison underscores our model's efficacy in image fusion, resulting in outstanding visual outcomes. As shown in Fig. 3, our method showcases superior visual quality compared to other approaches. Specifically, our method excels in preserving intricate texture details well lid in low light (Fig. 3 red box). Although TC-MoA and MUFusion approach our method in retaining details, they exhibit visible artifacts, blur, and low contrast—characteristics absent in CCF (Fig. 3, green box). CCF exhibits the highest contrast, the clearest details, and the most information content, further highlighting its superiority in preserving texture details. Its excellent detail retention and clear background generation further demonstrate the effectiveness of our proposed method.

5.2 Evaluation on Multi-Focus Fusion

For multi-focus image fusion, we compare our CCF with five general image fusion methods: U2Fusion [31], DeFusion [33], DDFM [24], Text-IF [47], and TC-MoA [34].

Quantitative Comparisons. We employ four quantitative metrics to evaluate our model, as shown in Table 2 (left). Our method significantly outperforms the comparison methods, achieving SOTA across all metrics. Specifically, the SD is 11.19 higher than the suboptimal value, indicating higher

7

Table 2: Comparison with SOTAs. The **red**/**blue**/**green** indicates the best, runner-up and third best.

	MFFW Dataset				MEFB Dataset			
	SD ↑	AG ↑	SF ↑	SCD ↑	SD ↑	AG ↑	SF ↑	SCD ↑
U2Fusion [31]	**67.83**	**8.08**	**22.19**	**2.67**	**64.88**	**5.56**	**18.74**	**2.05**
DeFusion [33]	54.75	4.76	12.72	0.50	52.75	4.32	14.12	−0.97
DDFM [24]	56.34	4.47	12.21	0.90	**67.30**	3.82	13.40	**2.12**
Text-IF [47]	**66.27**	**7.72**	**21.58**	**2.27**	62.51	4.78	**17.26**	1.46
TC-MoA [34]	57.55	6.95	20.67	1.03	50.27	**4.82**	15.64	0.42
CCF (ours)	**79.02**	**8.18**	**24.30**	**2.78**	**71.88**	**5.70**	**20.28**	**3.00**

contrast and clearer images. The SCD is 0.11 higher than the suboptimal value, suggesting a lower error between source images and fused images. The AG and SF also rank first demonstrating the retention of more texture details. These results showcase that our method effectively preserves details from the source images and produces high-quality fused images.

Qualitative Comparisons. As illustrated in Fig. 4, our proposed method demonstrates outstanding visual performance, particularly in preserving intricate details. We have carefully selected specific conditions that allow our approach to effectively handle the blurring caused by multi-focus scenes while retaining the original image's lighting and color information. In comparison, other DDPM-based methods such as DDFM are unable to achieve the same level of effectiveness as our approach. In Fig. 4 (red), our method excels in preserving the details of the watch hand. The closest result to ours is U2Fusion, but it loses texture and color fidelity, appearing blurry, in Fig. 4 (green). In short, our method performs well in maintaining both color and authentic details.

5.3 Evaluation on Multi-Exposure Fusion

For multi-exposure image fusion, we compare our model with five general image fusion methods, i.e., U2Fusion [31], DeFusion [33], DDFM [24], Text-IF [47], and TC-MoA [34].

Quantitative Comparisons. As demonstrated in Table 2 (right), our method achieved SOTA on the MEF index, analogous to the results observed for the MFF task. Notably, the metrics SD, AG, and SF signify the highest image quality, while SCD exhibits the highest correlation. Each of these metrics attained state-of-the-art performance levels, underscoring the efficacy of our approach. This consistent performance across multiple metrics illustrates the robustness and versatility of our method in enhancing image quality and fidelity.

Qualitative Comparisons. Fig. 4 demonstrates the excellent visual performance of our method. Our approach effectively addresses the issue of overexposure while preserving crucial details. In contrast, DDFM, which relies on finding the middle value of two images, struggles to maintain texture details. Similarly, Text-IF tends to result in higher average brightness, which can lead to content loss in overexposed scenes. Defusion and TC-MoA exhibit similar visual performance, with more blurred edges compared to our method. In comparison, our method strikes a balance between these challenges, resulting in superior visual fidelity and saturation compared to other existing methods.

5.4 Task-specific Conditions

The task-specific conditions can be manually selected. In this section, we use the detection condition as an example. The detection model employed is YOLOv5 [48], trained on the LLVIP dataset. We randomly select 287 images from the LLVIP test dataset to validate our method with the detection condition. Before adding the detection condition, the fused image achieved mAP.5 = 0.737, mAP.5 : .95 = 0.509, and a recall of 0.737. After incorporating the detection condition, the mAP.5 increased by 0.049 to 0.907, mAP.5 : .95 increased by 0.054 to 0.563, and recall significantly improved to 0.832. Fig. 5 visualizes several cases detected using YOLOv5.
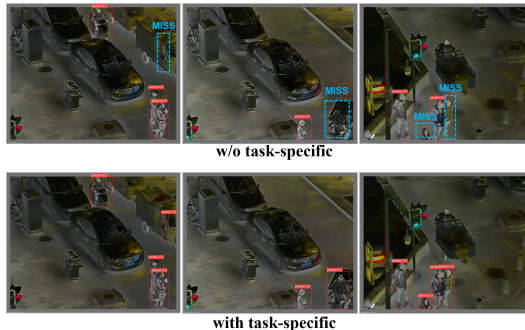

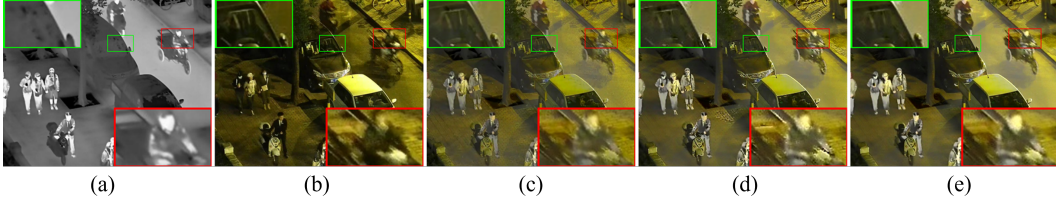Figure 5: The visualization of the w/o and with task-specific conditions.

Figure 6: Ablation study of condition bank. (a) is infrared image, (b) is visible image, (c) is basic condition, (d) is CCF w/o SCS, (e) is CCF.

The fused images with the detection condition exhibit higher confidence (columns 1 and 2) and recall (columns 1, 2, and 3). This demonstrates that task-specific conditions can enhance the performance of fused images in downstream tasks. By integrating task-specific conditions, the fused image can be precisely aligned with the demands of various applications, enhancing the overall effectiveness and utility of the generated images. More detail shows in App. F.

5.5 Ablation Study

Numerous ablation experiments were conducted to assess the effectiveness of different components of our model. The aforementioned four metrics were utilized to evaluate fusion performance across different experimental configurations. The quantitative results are presented in App. G.

To validate the effectiveness of the condition bank, we systematically add basic and enhanced conditions individually and then verify the effectiveness of SCS. Fig. 6 illustrates a gradual variation in performance metrics with the progressive addition of conditions.

In Fig. 6(a), using only the basic condition results in image fusion. When all enhanced conditions are injected together without SCS, the metrics all reduced (Fig. 6(b)), likely due to the conflict between different conditions, as evidenced by the messy lines and random noise in Fig. 6(d). This demonstrates that injecting conditions unevenly without DCS leads to suboptimal results. After introducing DCS, both the metrics and visual results (Fig. 6(e)) are well-balanced, with conditions being injected as needed during the generation process. This indicates the effectiveness of the condition bank and DCS in dynamically and appropriately selecting the conditions.

5.6 Discussion on Controllable Fusion

Our method enables the dynamic selection of conditions, allowing for the adaptive customization of conditions for each sample. As illustrated in Fig. 1, the statistics show the condition selection at various diffusion sampling stages. Initially, the process is stochastic due to random noise (around 0 to $\frac{1}{4}T$ steps). As denoising progresses, the content of the image starts to be dominant in fusion, and conditions like MSE, SSIM, and SD are most frequently chosen (around $\frac{1}{4}T$ to $\frac{3}{4}T$ steps). As the process continues, and the fusion model tends to generate more texture details, conditions like EI and edge become more dominant (around $\frac{3}{4}T$ to T steps). SSIM also remains selected to constrain the structure, whereas the frequency of SD selection decreases. This demonstrates the crucial role of dynamically selecting conditions during the diffusion sampling process. Our CCF adaptively decomposes diverse conflict fusion conditions into different denoising steps, which is significantly compatible with the reconstruction preferences of different steps in the denoising model. This dynamic fusion paradigm ensures appropriate condition selection at each stage of the sampling.

6 Conclusion

In this paper, we introduce a learning-free approach for conditional controllable image fusion (CCF), utilizing a condition bank to regulate joint information with a pre-trained DDPM. We capitalize on the remarkable reconstruction abilities of DDPM and integrate them into the sampling steps. Sample-adaptive condition selection facilitates fusion in dynamic scenarios. Varied fusion images can personalize their conditions to emphasize different aspects. Empirical findings demonstrate that CCF surpasses the competing methods in achieving superior performance for general image fusion tasks. In the future, we will further explore automatic manners to distinguish basic and enhanced conditions to reduce empirical intervention, thereby enabling more robust and reliable image fusion.

Acknowledgements.

References

[1] Shutao Li, Xudong Kang, Leyuan Fang, Jianwen Hu, and Haitao Yin. Pixel-level image fusion: A survey of the state of the art. *information Fusion*, 33:100–112, 2017.

[2] Jiaxin Li, Danfeng Hong, Lianru Gao, Jing Yao, Ke Zheng, Bing Zhang, and Jocelyn Chanussot. Deep learning in multimodal remote sensing data fusion: A comprehensive review. *International Journal of Applied Earth Observation and Geoinformation*, 112:102926, 2022.

[3] Xingchen Zhang, Ping Ye, and Gang Xiao. Vifb: A visible and infrared image fusion benchmark. In *Proceedings of the IEEE/CVF Conference on Computer Vision and Pattern Recognition Workshops*, pages 104–105, 2020.

[4] Fang Xu, Jinghong Liu, Yueming Song, Hui Sun, and Xuan Wang. Multi-exposure image fusion techniques: A comprehensive review. *Remote Sensing*, 14(3):771, 2022.

[5] Jinyuan Liu, Jingjie Shang, Risheng Liu, and Xin Fan. Attention-guided global-local adversarial learning for detail-preserving multi-exposure image fusion. *IEEE Transactions on Circuits and Systems for Video Technology*, 32(8):5026–5040, 2022.

[6] Yu Liu, Lei Wang, Juan Cheng, Chang Li, and Xun Chen. Multi-focus image fusion: A survey of the state of the art. *Information Fusion*, 64:71–91, 2020.

[7] Bing Cao, Yiming Sun, Pengfei Zhu, and Qinghua Hu. Multi-modal gated mixture of local-to-global experts for dynamic image fusion. In *Proceedings of the IEEE/CVF International Conference on Computer Vision (ICCV)*, pages 23555–23564, October 2023.

[8] Yiming Sun, Bing Cao, Pengfei Zhu, and Qinghua Hu. Detfusion: A detection-driven infrared and visible image fusion network. In *Proceedings of the 30th ACM International Conference on Multimedia*, pages 4003–4011, 2022.

[9] Chenxiao Zhang, Peng Yue, Deodato Tapete, Liangcun Jiang, Boyi Shangguan, Li Huang, and Guangchao Liu. A deeply supervised image fusion network for change detection in high resolution bi-temporal remote sensing images. *ISPRS Journal of Photogrammetry and Remote Sensing*, 166:183–200, 2020.

[10] Jinyuan Liu, Xin Fan, Zhanbo Huang, Guanyao Wu, Risheng Liu, Wei Zhong, and Zhongxuan Luo. Target-aware dual adversarial learning and a multi-scenario multi-modality benchmark to fuse infrared and visible for object detection. In *Proceedings of the IEEE/CVF Conference on Computer Vision and Pattern Recognition*, pages 5802–5811, 2022.

[11] Chaoben Du and Shesheng Gao. Image segmentation-based multi-focus image fusion through multi-scale convolutional neural network. *IEEE access*, 5:15750–15761, 2017.

[12] Jinyuan Liu, Zhu Liu, Guanyao Wu, Long Ma, Risheng Liu, Wei Zhong, Zhongxuan Luo, and Xin Fan. Multi-interactive feature learning and a full-time multi-modality benchmark for image fusion and segmentation. In *Proceedings of the IEEE/CVF International Conference on Computer Vision*, pages 8115–8124, 2023.

[13] Abeer D Algarni. Automated medical diagnosis system based on multi-modality image fusion and deep learning. *Wireless Personal Communications*, 111:1033–1058, 2020.

[14] Yiming Sun, Bing Cao, Pengfei Zhu, and Qinghua Hu. Detfusion: A detection-driven infrared and visible image fusion network. In *Proceedings of the 30th ACM International Conference on Multimedia*, 2022.

[15] Han Xu and Jiayi Ma. Emfusion: An unsupervised enhanced medical image fusion network. *Information Fusion*, 76:177–186, 2021.

[16] Kanika Bhalla, Deepika Koundal, Bhisham Sharma, Yu-Chen Hu, and Atef Zaguia. A fuzzy convolutional neural network for enhancing multi-focus image fusion. *Journal of Visual Communication and Image Representation*, 84:103485, 2022.

[17] Han Xu, Jiayi Ma, and Xiao-Ping Zhang. Mef-gan: Multi-exposure image fusion via generative adversarial networks. *IEEE Transactions on Image Processing*, 29:7203–7216, 2020.

[18] Krista Amolins, Yun Zhang, and Peter Dare. Wavelet based image fusion techniques—an introduction, review and comparison. *ISPRS Journal of photogrammetry and Remote Sensing*, 62(4):249–263, 2007.

[19] Yu Liu, Xun Chen, Hu Peng, and Zengfu Wang. Multi-focus image fusion with a deep convolutional neural network. *Information Fusion*, 36:191–207, 2017.

[20] Jinyuan Liu, Runjia Lin, Guanyao Wu, Risheng Liu, Zhongxuan Luo, and Xin Fan. Coconet: Coupled contrastive learning network with multi-level feature ensemble for multi-modality image fusion. *International Journal of Computer Vision*, 132(5):1748–1775, 2024.

[21] Jiayi Ma, Wei Yu, Chen Chen, Pengwei Liang, Xiaojie Guo, and Junjun Jiang. Pan-gan: An unsupervised pan-sharpening method for remote sensing image fusion. *Information Fusion*, 62: 110–120, 2020.

[22] Jooyoung Choi, Sungwon Kim, Yonghyun Jeong, Youngjune Gwon, and Sungroh Yoon. Ilvr: Conditioning method for denoising diffusion probabilistic models. In *2021 IEEE/CVF International Conference on Computer Vision (ICCV)*, 2021.

[23] Mining Li, Ronghao Pei, Tianyou Zheng, Yang Zhang, and Weiwei Fu. Fusiondiff: Multi-focus image fusion using denoising diffusion probabilistic models. *Expert Systems with Applications*, 238:121664, 2024.

[24] Zixiang Zhao, Haowen Bai, Yuanzhi Zhu, Jiangshe Zhang, Shuang Xu, Yulun Zhang, Kai Zhang, Deyu Meng, Radu Timofte, and Luc Van Gool. Ddfm: denoising diffusion model for multi-modality image fusion. *arXiv preprint arXiv:2303.06840*, 2023.

[25] Jinyuan Liu, Xin Fan, Ji Jiang, Risheng Liu, and Zhongxuan Luo. Learning a deep multi-scale feature ensemble and an edge-attention guidance for image fusion. *IEEE Transactions on Circuits and Systems for Video Technology*, 32(1):105–119, 2021.

[26] Hui Li, Xiao-Jun Wu, and Josef Kittler. Infrared and visible image fusion using a deep learning framework. In *2018 24th international conference on pattern recognition (ICPR)*, pages 2705–2710. IEEE, 2018.

[27] Mostafa Amin-Naji, Ali Aghagolzadeh, and Mehdi Ezoji. Ensemble of cnn for multi-focus image fusion. *Information fusion*, 51:201–214, 2019.

[28] Yu Liu, Xun Chen, Juan Cheng, and Hu Peng. A medical image fusion method based on convolutional neural networks. In *2017 20th international conference on information fusion (Fusion)*, pages 1–7. IEEE, 2017.

[29] Jiayi Ma, Chen Chen, Chang Li, and Jun Huang. Infrared and visible image fusion via gradient transfer and total variation minimization. *Information Fusion*, page 100–109, Sep 2016.

[30] Zixiang Zhao, Haowen Bai, Jiangshe Zhang, Yulun Zhang, Shuang Xu, Zudi Lin, Radu Timofte, and Luc Van Gool. Cddfuse: Correlation-driven dual-branch feature decomposition for multi-modality image fusion. In *Proceedings of the IEEE/CVF conference on computer vision and pattern recognition*, pages 5906–5916, 2023.

[31] Han Xu, Jiayi Ma, Junjun Jiang, Xiaojie Guo, and Haibin Ling. U2fusion: A unified unsupervised image fusion network. *IEEE Transactions on Pattern Analysis and Machine Intelligence*, 44(1):502–518, 2020.

[32] Jiayi Ma, Linfeng Tang, Fan Fan, Jun Huang, Xiaoguang Mei, and Yong Ma. Swinfusion: Cross-domain long-range learning for general image fusion via swin transformer. *IEEE/CAA Journal of Automatica Sinica*, 9(7):1200–1217, 2022.

[33] Pengwei Liang, Junjun Jiang, Xianming Liu, and Jiayi Ma. Fusion from decomposition: A self-supervised decomposition approach for image fusion. In *European Conference on Computer Vision*, pages 719–735. Springer, 2022.

[34] Pengfei Zhu, Yang Sun, Bing Cao, and Qinghua Hu. Task-customized mixture of adapters for general image fusion. *arXiv preprint arXiv:2403.12494*, 2024.

[35] Jonathan Ho, Ajay Jain, and Pieter Abbeel. Denoising diffusion probabilistic models. *Advances in neural information processing systems*, 33:6840–6851, 2020.

[36] Yang Song, Jascha Sohl-Dickstein, Diederik P Kingma, Abhishek Kumar, Stefano Ermon, and Ben Poole. Score-based generative modeling through stochastic differential equations. *arXiv preprint arXiv:2011.13456*, 2020.

[37] Prafulla Dhariwal and Alexander Nichol. Diffusion models beat gans on image synthesis. *Advances in neural information processing systems*, 34:8780–8794, 2021.

[38] Hyungjin Chung, Jeongsol Kim, Michael T Mccann, Marc L Klasky, and Jong Chul Ye. Diffusion posterior sampling for general noisy inverse problems. *arXiv preprint arXiv:2209.14687*, 2022.

[39] Hyungjin Chung, Jeongsol Kim, MichaelT. Mccann, MarcL. Klasky, and JongChul Ye. Diffusion posterior sampling for general noisy inverse problems. *The Eleventh International Conference on Learning Representations*, Sep 2023.

[40] Zhao Chen, Vijay Badrinarayanan, Chen-Yu Lee, and Andrew Rabinovich. Gradnorm: Gradient normalization for adaptive loss balancing in deep multitask networks. In *International conference on machine learning*, pages 794–803. PMLR, 2018.

[41] Xinyu Jia, Chuang Zhu, Minzhen Li, Wenqi Tang, and Wenli Zhou. Llvip: A visible-infrared paired dataset for low-light vision. In *Proceedings of the IEEE/CVF international conference on computer vision*, pages 3496–3504, 2021.

[42] Xingchen Zhang. Benchmarking and comparing multi-exposure image fusion algorithms. *Information Fusion*, 74:111–131, 2021.

[43] Xingchen Zhang. Deep learning-based multi-focus image fusion: A survey and a comparative study. *IEEE Transactions on Pattern Analysis and Machine Intelligence*, 44(9):4819–4838, 2021.

[44] Prafulla Dhariwal and AlexanderQuinn Nichol. Diffusion models beat gans on image synthesis. *Neural Information Processing Systems,Neural Information Processing Systems*, Dec 2021.

[45] Linfeng Tang, Xinyu Xiang, Hao Zhang, Meiqi Gong, and Jiayi Ma. Divfusion: Darkness-free infrared and visible image fusion. *Information Fusion*, 91:477–493, 2023.

[46] Chunyang Cheng, Tianyang Xu, and Xiao-Jun Wu. Mufusion: A general unsupervised image fusion network based on memory unit. *Information Fusion*, 92:80–92, 2023.

[47] Xunpeng Yi, Han Xu, Hao Zhang, Linfeng Tang, and Jiayi Ma. Text-if: Leveraging semantic text guidance for degradation-aware and interactive image fusion. *arXiv preprint arXiv:2403.16387*, 2024.

[48] Glenn Jocher. Yolov5 by ultralytics, 2020. URL https://github.com/ultralytics/yolov5. doi:10.5281/zenodo.3908559.

[49] Wenlong Zhang, Xiaolin Liu, Wuchao Wang, and Yujun Zeng. Multi-exposure image fusion based on wavelet transform. *International Journal of Advanced Robotic Systems*, 15(2):1729881418768939, 2018.

[50] Jianming Zhang, Mingshuang Wu, Wei Cao, and Zi Xing. Partition-based image exposure correction via wavelet-based high frequency restoration. In *International Conference on Intelligent Computing*, pages 452–463. Springer, 2024.

[51] Linfeng Tang, Hao Zhang, Han Xu, and Jiayi Ma. Rethinking the necessity of image fusion in high-level vision tasks: A practical infrared and visible image fusion network based on progressive semantic injection and scene fidelity. *Information Fusion*, page 101870, 2023.

[52] Hui Li and Xiao-Jun Wu. Densefuse: A fusion approach to infrared and visible images. *IEEE Transactions on Image Processing*, 28(5):2614–2623, 2018.

[53] Hui Li, Xiao-Jun Wu, and Josef Kittler. Rfn-nest: An end-to-end residual fusion network for infrared and visible images. *Information Fusion*, 73:72–86, 2021.

[54] Di Wang, Jinyuan Liu, Xin Fan, and Risheng Liu. Unsupervised misaligned infrared and visible image fusion via cross-modality image generation and registration. *arXiv preprint arXiv:2205.11876*, 2022.

[55] Wei Tang, Fazhi He, and Yu Liu. Ydtr: Infrared and visible image fusion via y-shape dynamic transformer. *IEEE Transactions on Multimedia*, 2022.

[56] Linfeng Tang, Jiteng Yuan, Hao Zhang, Xingyu Jiang, and Jiayi Ma. Piafusion: A progressive infrared and visible image fusion network based on illumination aware. *Information Fusion*, 83: 79–92, 2022.

[57] Tim Salimans, Andrej Karpathy, Xi Chen, and Diederik P Kingma. Pixelcnn++: Improving the pixelcnn with discretized logistic mixture likelihood and other modifications. *arXiv preprint arXiv:1701.05517*, 2017.

[58] Ashish Vaswani, Noam Shazeer, Niki Parmar, Jakob Uszkoreit, Llion Jones, Aidan N Gomez, Łukasz Kaiser, and Illia Polosukhin. Attention is all you need. *Advances in neural information processing systems*, 30, 2017.

[59] Alex Pappachen James and Belur V Dasarathy. Medical image fusion: A survey of the state of the art. *Information fusion*, 19:4–19, 2014.

[60] Keith A. Johnson and J. Alex Becker. Harvard medical website, 2023. URL `http://www.med.harvard.edu/AANLIB/home.html`.

Appendix

A Experimental Settings

Our method not only excels in individual settings to generate customized images but also demonstrates robust performance in general settings. In this section, we elaborate on numerous experiments for image fusion tasks to demonstrate the superiority of our method. For different tasks, the basic conditions vary. Specifically, in the VIF task, MSE [24, 46, 31, 34] serves as the basic condition, where c_{MSE} can be expressed as $||\text{MSE}(i, x_0) + \text{MSE}(v, x_0)||$. In contrast, for the MEF and MFF tasks, to achieve clearer and higher fidelity images and inspired by [29, 6, 49, 50], the basic conditions include MSE, frequency and edge conditions, as detailed in the App. C. To ensure convenience and fairness, we select eight enhanced conditions from the condition bank: SSIM, MSE, Edge, Low-frequency, High-frequency, Spatial Frequency, Edge Intensity, and Standard Deviation while setting $k = 3$ across all tasks.

B Experiments on More Comparisons

In our evaluation using the TNO dataset, we referred to the test set outlined in the work by Tang et al. [51] We evaluated the fusion results in both quantitative and qualitative. Qualitative evaluation primarily hinges on subjective visual assessments conducted by individuals. We expect that the fused image will exhibit rich texture details and abundant color saturability. For different task scenarios, the different evaluation metrics used, specifically, we employ six metrics including standard deviation (SD), entropy (EN), spatial frequency (SF), sum of the correlations of differences (SCD), Structural Similarity (SSIM), and edge intensity (EI). In the MFF and MEF tasks, considering the different task scenarios, we employ SD, AG, SF, SCD, and MSE for evaluation metrics. For multi-modal image fusion, we compare our method with four task-specific methods: DenseFuse [52], RFN-Nest [53], UMF-CMGR [54], YDTR [55], and three general approaches U2Fusion [31], DeFusion [33]and DDFM [24] on the LLVIP dataset and TNO dataset.

Quantitative Comparisons. We employ 6 quantitative metrics to evaluate our model, as shown in Table 3. Our method demonstrated exceptional performance across various evaluation metrics. On the TNO dataset, our method achieves the best result on the SD, EN, and SCD indicators. The result shows suboptimal performance in SF and is close to the best values. Notably, our method does not necessitate turning and holds its ground against methods requiring training. Compared with the learning-free DDFM and DeFusion, our method shows better results. This demonstrates the excellent performance of our model, achieving high performance across almost all indicators in a tuning-free model.

Qualitative Comparisons. The incorporation of both basic and enhanced conditions enables effective preservation of background and texture. This comparison underscores our model's efficacy in image fusion, resulting in outstanding visual outcomes. As shown in Fig.7, our method demonstrates superior visual quality compared to other approaches. Specifically, it excels in preserving intricate texture details and color fidelity, such as license plate numbers (highlighted in the red box in Fig.7). The DDFM and DeFusion approaches retain fewer texture details. As depicted in Fig. 7, CCF exhibits the highest contrast, the clearest details, and the most comprehensive information content, further highlighting its superiority in preserving texture details. Its excellent detail retention ability and clear background generation further prove the effectiveness of our proposed method.

C Basic Conditions of the MEF and MFF

High-frequency It's commonly understood that the high-frequency information in both modalities is distinctive to each modality. For instance, texture and detailed information are specific to visible images, while thermal radiation information pertains to infrared images. Specifically, we utilizes wavelet transform to extract high-frequency information from the image. For example, 2D discrete wavelet transformation with Haar wavelets to transform the input image (IM) into four sub-bands can be expressed as:

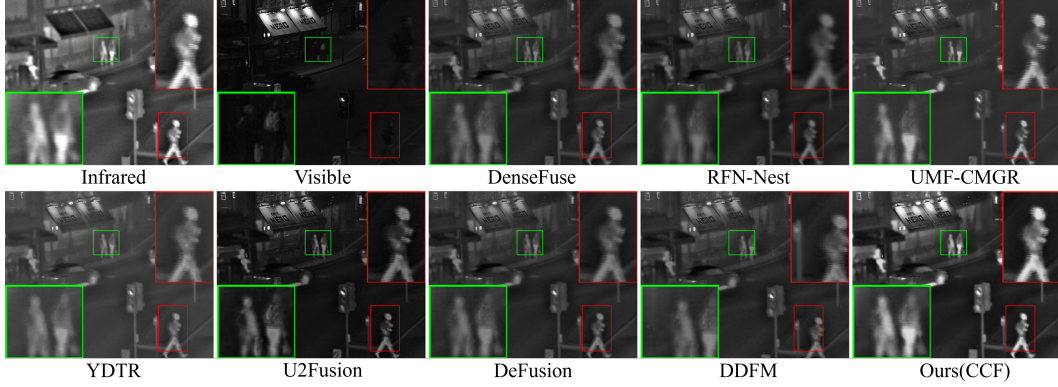$$\{LL_k, HL_k, LH_k, HH_k\} = \mathcal{W}_k(LL_{k-1}) \tag{14}$$

Figure 7: Qualitative comparisons of our CCF and the competing methods on VIF fusion task of TNO dataset

where $LL_k, HL_k, LH_k, HH_k \in \mathcal{R}^{\frac{H}{2^k} \times \frac{W}{2^k} \times c}, k \in [1, K]$, signify the averages of the input image and the high-frequency details in the vertical, horizontal, and diagonal directions, respectively, at the first-level wavelet decomposition. Denote that the high-frequency details $H_F(\text{IM})$ from IM. So we can see the high-frequency condition below:

$$\widetilde{HF} = H_F(x_0) - F(\lambda_h |H_F(i)|, (1 - \lambda_h)|H_F(v)|) \tag{15}$$

where $|\cdot|$ stands for the absolute operation and $F(\cdot, \cdot)$ can represent a variety of customized functions. In this paper, specifically, we employ the max function. The restored average coefficient and the high-frequency coefficient at scale k are correspondingly converted into the output at scale $k - 1$ by employing $\mathcal{W}^{-1}$ the 2D inverse discrete wavelet transform:

$$\delta_{c_h} = \mathcal{W}^{-1}\{LL_k, \widetilde{HF}_k\} \tag{16}$$

Low-Frequency Condition. Low-frequency components generally encapsulate information common to both modes. For simplicity, we directly utilize the low-frequency information obtained via wavelet transform. However, each mode may possess slightly varying amounts of low-frequency information. Our conditions allow for the adjustment of the low-frequency L_F fusion ratio with hyperparameters, i.e.,

$$\widetilde{LL} = L_F(x_0) - (\lambda_l L_F(i) + (1 - \lambda_l)L_F(v)) \tag{17}$$

$$\delta_{c_l} = \mathcal{W}^{-1}\{\widetilde{LL}_k, HF_k\} \tag{18}$$

Edge Condition. We aim at the fused image to retain the more intricate texture details from both infrared and visible images. To achieve this, we integrated edge conditions into the set of conditions

Table 3: Comparison with SOTAs. **Red** indicates the best, **blue** indicates the second best, and **green** indicates the third best.

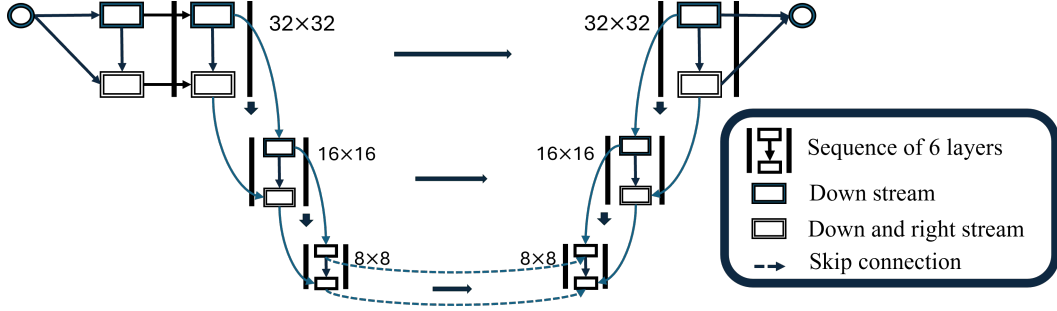|	TNO Dataset					
	SD ↑	EN ↑	SF ↑	SSIM ↑	SCD ↑	EI↑
DenseFuse [52]	34.83	6.82	8.99	1.38	1.78	8.75
RFN-Nest [53]	36.90	6.96	5.87	1.31	1.78	7.13
UMF-CMGR [54]	29.97	6.53	8.17	1.43	1.64	7.32
YDTR [55]	28.03	6.43	7.62	1.41	1.56	6.81
U2Fusion [56]	37.70	7.00	11.86	1.28	1.78	12.78
DeFusion [31]	30.38	6.58	6.20	1.38	1.53	6.54
DDFM [24]	34.45	6.85	7.27	1.08	1.54	7.89
CCF (ours)	40.11	7.01	10.20	1.38	1.84	8.29

Figure 8: Framework of our neural network architecture.

to enhance the edge texture in the fused image. The condition is defined as :

$$\delta_{c_e} = |\nabla(x_0)| - F(\lambda_e|\nabla(i)|, (1-\lambda_e)|\nabla(v)|) \tag{19}$$

where ∇ indicates the Sobel gradient operator, which measures the texture detail information of an image.

MSE Condition. We incorporate the information from the original image into the fused image as a supplementary content condition. Essentially, we utilize the image reconstruction capability of DDPM to supplement lost details and enhance the informational content pertaining to the target in the fused image, i.e.

$$\delta_{c_{MSE}} = x_0 - \Psi^{-1}(\lambda_{MSE}\Psi(x_0) - (1-\lambda_{MSE})\Psi(y)) \tag{20}$$

where Ψ and Ψ^{-1} represent the downsample and upsample operator, respectively, while y can refer to either the infrared or visible image.

Totally, these conditions can be combined to govern the generation of the final fused image:

$$\delta_c = \eta_h \delta_{c_h} + \eta_l \delta_{c_l} + \eta_e \delta_{c_e} + \eta_{cont} \delta_{c_{MSE}} \tag{21}$$

D More Details of CCF

In the sampling process, the neural network architecture is similar to PixelCNN++ [57], consisting of a U-Net backbone with group normalization. The diffusion step t is defined by incorporating the Transformer [58] sinusoidal position embedding into each residual block. As shown in Fig. 8, six feature map resolutions are utilized, with two convolutional residual blocks per resolution level. Additionally, self-attention blocks are incorporated at the 16×16 resolution between the convolutional blocks.

Representing a process of reverse diffusion (sampling), starting from a standard normal distribution $\mathcal{N}(0, I)$, T sampling steps are performed

---

Algorithm 1 CCF

Input: : i,v
Output: : f
1: $\delta_C \leftarrow C(i,v)$
2: Sample $x_T \sim \mathcal{N}(0, I)$
3: **for** t=T, .., 1 **do**
4:     $z \sim \mathcal{N}(0, I)$
5:     $x_0 = \frac{x_t - \sqrt{1-\bar{\alpha}_t}\epsilon_\theta(x_{t-1}|x_t)}{\sqrt{\bar{\alpha}_t}}$
6:     **for** k=N,..., 1 **do**
7:        $\hat{x}_0 \leftarrow x_0 - \lambda \bigtriangledown \delta_{c_k}$
8:     **end for**
9: **end for**

---

to generate the final fused image. However, the generation with unconditional DDPM [35] is uncontrollable. Therefore, conditions selected from the condition bank we constructed are introduced to control the sampling process. More precisely, the conditions can rectify each step's estimation of x_0. Finally, after the T step, the final fused image can be generated. The algorithm of CCF is presented in Algorithm 1.

E More About Enhanced Conditions

We follow the recent works [30, 24, 46], and adopt the eight most commonly used constraints as conditions in this paper. However, as shown in Table 4, our approach is not restricted to these

Table 4: Comparison across different numbers of enhancement conditions. For the 4 conditions, conditions include SSIM, MSE, Edge, and SD. The 8 conditions expand to include SSIM, MSE, Edge, SD, Low-frequency, High-frequency, SF, and EI. The 12 conditions incorporate the previous 8 conditions with four additional conditions: CC, MMS-SSIM, SCD, and VIF. **Bold** indicates the best results

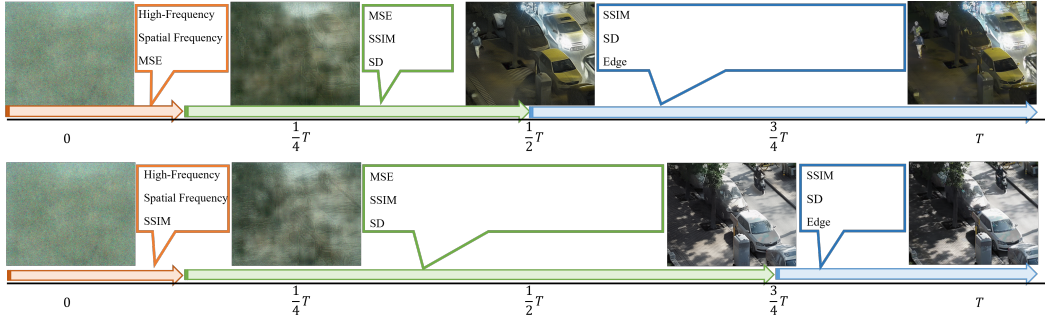| Number of conditions	SSIM ↑	MSE ↓	CC ↑	PSNR ↑	Nabf ↓	Avg. Runtime(s)
4	1.12	1820	0.699	32.20	0.034	188
8 (ours)	**1.22**	1694	0.705	32.58	0.005	222
12	1.20	**1545**	**0.719**	**33.21**	**0.002**	454

Figure 9: Example of enhanced conditions selection in denoising iteration for rapidly changing scenarios.

constraints; fewer conditions can be randomly selected (here we select SSIM, MSE, Edge, and SD), and additional enhanced conditions [31, 34](Correlation Coefficient (CC), Multi-Scale Structural Similarity (MS-SSIM), the Sum of the Correlations of Differences (SCD), and the Visual Information Fidelity (VIF)) can also be incorporated. Additionally, we evaluate the runtime across different numbers of conditions to assess their impact on efficiency. While adding more conditions slightly improves performance, it also increases inference runtime.

Fig. 9 illustrates the selection of enhanced conditions at each denoising step in the same location under both daylight and nighttime scenarios, representing a typical rapidly changing environment. It demonstrates that CCF can adapt to these changing environments by selecting different conditions at various denoising steps to respond effectively to dynamic environmental characteristics.

F More About Task-specific Conditions

The task-specific conditions are incorporated to guide the fusion process throughout the denoising procedure. For instance, we take the Euclidean distance of features extracted by the object detection model as the detection condition. In our experiments, we employ YOLOv5, which is pretrained on the visible modality, to extract features from both the estimated x_0 at each step and the visible image. The Euclidean distance is minimized in the inverse diffusion process iteratively. Consequently, the final fused image progressively integrates the object-specific information, enhancing the fusion performance. We provide additional visualizations of the detection conditions, as shown in Fig. 10, directly fused images appear to have a lot of missed detection in raw 1-4 and the detection scores are generally higher. The last row of Fig.10 demonstrates a reduction in false-positive boxes when the detection condition is applied.

Table 5 also supports this, indicating that metrics such as mAP.5, mAP.5:95, and recall have increased remarkably, showing that our method can customize conditions to fit the downstream task effectively. By tailoring conditions to specific tasks, our approach effectively improves the applicability of fused images for particular applications, as evidenced by the improved detection metrics. We further explored the use of different levels of features obtained with YoloV5 as detection conditions. Specifically, we evaluate in three scales and each of the scales is evaluated individually, and all features combined involve using all three scale features simultaneously, averaged, to add task-specific perception to enhance task performance. Furthermore, Table 5 indicates that there is no significant

17

Table 5: Comparison of task-specific conditions across different scales of features in YOLOv5s. The **Bold** indicates the best results.

Scale of feature	Position	mAP.5	mAP.5:95	Recall
w/o Feature	-	0.858	0.509	0.737
Feature 1 (160×128)	Before	0.884	0.537	0.832
Feature 2 (80×64)	Before	0.890	0.540	0.826
Feature 3 (40×32) (ours)	Before	**0.907**	**0.563**	0.832
All Features ($\frac{1}{3}\sum_3^i$ Feature i)	Before	0.882	0.541	**0.837**
Final performance	After	0.894	0.537	0.824

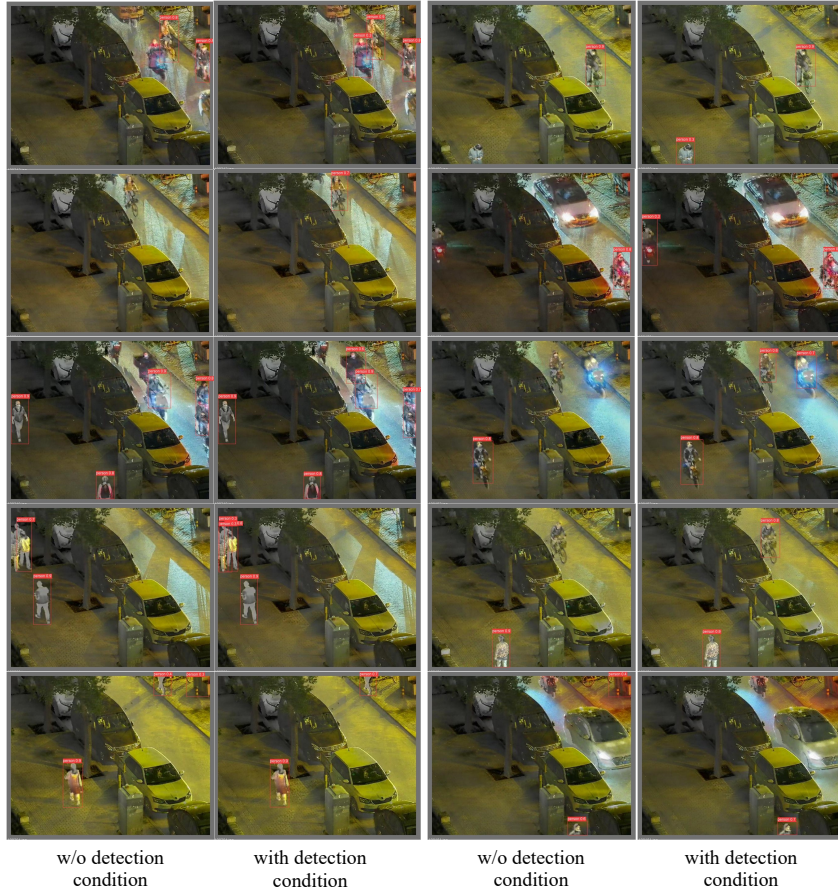| w/o detection condition | with detection condition | w/o detection condition | with detection condition |

Figure 10: Qualitative Comparisons of w/o and with the detection condition.

difference between using different features. The constraint primarily enhances the implicit expressive ability of the image, enabling it to better adapt to downstream tasks.

G Ablation

The quantitative results of the ablation study compare different scenarios: without DDPM, with only basic conditions, with enhanced conditions but without SCS, and the complete CCF results. With the reconstruction capability of DDPM, the fusion performance significantly improved after the conditions were integrated. Some metrics for the enhanced conditions without SCS show a decline due to conflicts among the various focusing aspect conditions. However, after incorporating SCS, most metrics improve, demonstrating that SCS can enhance the image fusion process, producing high-quality images.

Table 6: Ablation studies on the LLVIP dataset. **Bold** indicates the best.

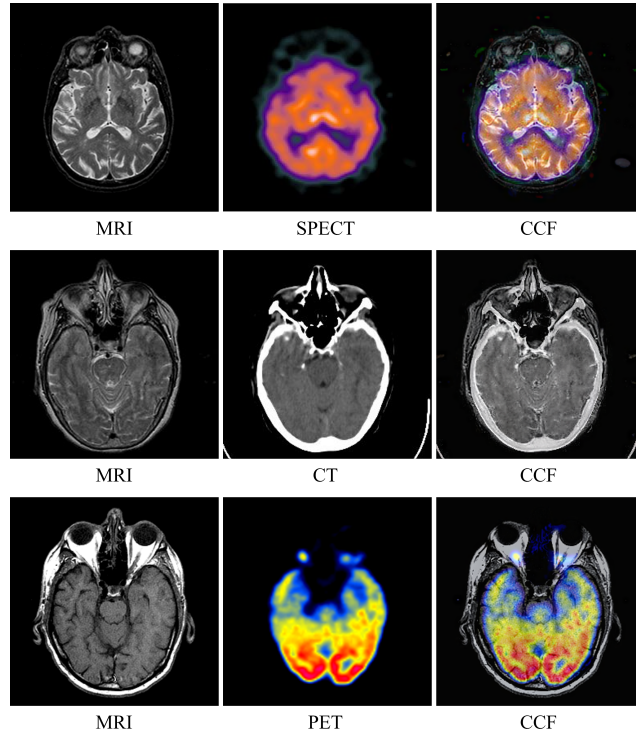| DDPM	Basic Conditions	Enhanced conditions	SCS	SSIM↑	MSE↓	CC↑	PSNR↑	Nabf↓
✓				0.28	2947	0.452	27.64	0.131
✓	✓			1.16	1785	0.683	**33.06**	0.032
✓	✓	✓		1.16	1779	0.677	32.17	0.072
✓	✓	✓	✓	**1.22**	**1694**	**0.705**	32.58	**0.005**

Figure 11: Visualization of medical image fusion.

H   Experiments on Medical Image Fusion

Medical image fusion (MIF)[59] experiments were conducted to validate the efficacy of our proposed method using the Harvard Medical Image Dataset[60]. We visualized fused medical images, focusing on MRI-SPECT, MRI-CT, and MRI-PET fusion, with the results presented in Fig. 11. Observing our fused images, it is evident that the preservation of both the skull's shape and intensity is notably well-maintained. Within the brain region, the CCF method effectively combines intricate details and structures from the two modalities.

I   Limitations and Broader Impacts

Even though the proposed CCF model achieves superior performance over existing methods and demonstrates advanced generalization with dynamic condition selection, there are still some potential limitations. We provide a condition bank, but it needs to be constructed empirically. Most of the conditions are inspired by Image Quality Assessment (IQA), but classifying these conditions is challenging due to the complexity of IQA. Therefore, it is necessary to propose a method to automatically classify the conditions, reducing empirical intervention. Additionally, our method relies on a pre-trained diffusion model, which limits its efficiency and makes the generation process time-consuming. Exploring more effective sampling processes would be valuable to improve efficiency and further enhance the model's performance. For potential social impact, it is difficult to ensure the effectiveness of selected conditions for all scenarios, which may be risky in high-risk scenarios such as medical imaging and autonomous driving.

NeurIPS Paper Checklist

1. **Claims**

   Question: Do the main claims made in the abstract and introduction accurately reflect the paper's contributions and scope?

   Answer: [Yes]

   Justification: The main claims made in the abstract and introduction accurately reflect the contributions and scope.

   Guidelines:

   - The answer NA means that the abstract and introduction do not include the claims made in the paper.
   - The abstract and/or introduction should clearly state the claims made, including the contributions made in the paper and important assumptions and limitations. A No or NA answer to this question will not be perceived well by the reviewers.
   - The claims made should match theoretical and experimental results, and reflect how much the results can be expected to generalize to other settings.
   - It is fine to include aspirational goals as motivation as long as it is clear that these goals are not attained by the paper.

2. **Limitations**

   Question: Does the paper discuss the limitations of the work performed by the authors?

   Answer: [Yes]

   Justification: The limitation is discussed in the App. I.

   Guidelines:

   - The answer NA means that the paper has no limitation while the answer No means that the paper has limitations, but those are not discussed in the paper.
   - The authors are encouraged to create a separate "Limitations" section in their paper.
   - The paper should point out any strong assumptions and how robust the results are to violations of these assumptions (e.g., independence assumptions, noiseless settings, model well-specification, asymptotic approximations only holding locally). The authors should reflect on how these assumptions might be violated in practice and what the implications would be.
   - The authors should reflect on the scope of the claims made, e.g., if the approach was only tested on a few datasets or with a few runs. In general, empirical results often depend on implicit assumptions, which should be articulated.
   - The authors should reflect on the factors that influence the performance of the approach. For example, a facial recognition algorithm may perform poorly when image resolution is low or images are taken in low lighting. Or a speech-to-text system might not be used reliably to provide closed captions for online lectures because it fails to handle technical jargon.
   - The authors should discuss the computational efficiency of the proposed algorithms and how they scale with dataset size.
   - If applicable, the authors should discuss possible limitations of their approach to address problems of privacy and fairness.
   - While the authors might fear that complete honesty about limitations might be used by reviewers as grounds for rejection, a worse outcome might be that reviewers discover limitations that aren't acknowledged in the paper. The authors should use their best judgment and recognize that individual actions in favor of transparency play an important role in developing norms that preserve the integrity of the community. Reviewers will be specifically instructed to not penalize honesty concerning limitations.

3. **Theory Assumptions and Proofs**

   Question: For each theoretical result, does the paper provide the full set of assumptions and a complete (and correct) proof?

   Answer: [NA]

Justification: This paper does not provide theoretical results.

Guidelines:

- The answer NA means that the paper does not include theoretical results.
- All the theorems, formulas, and proofs in the paper should be numbered and cross-referenced.
- All assumptions should be clearly stated or referenced in the statement of any theorems.
- The proofs can either appear in the main paper or the supplemental material, but if they appear in the supplemental material, the authors are encouraged to provide a short proof sketch to provide intuition.
- Inversely, any informal proof provided in the core of the paper should be complemented by formal proofs provided in appendix or supplemental material.
- Theorems and Lemmas that the proof relies upon should be properly referenced.

4. **Experimental Result Reproducibility**

Question: Does the paper fully disclose all the information needed to reproduce the main experimental results of the paper to the extent that it affects the main claims and/or conclusions of the paper (regardless of whether the code and data are provided or not)?

Answer: [Yes]

Justification: We provide implementation details in Sec. 5 and experimental setting in App. A.

Guidelines:

- The answer NA means that the paper does not include experiments.
- If the paper includes experiments, a No answer to this question will not be perceived well by the reviewers: Making the paper reproducible is important, regardless of whether the code and data are provided or not.
- If the contribution is a dataset and/or model, the authors should describe the steps taken to make their results reproducible or verifiable.
- Depending on the contribution, reproducibility can be accomplished in various ways. For example, if the contribution is a novel architecture, describing the architecture fully might suffice, or if the contribution is a specific model and empirical evaluation, it may be necessary to either make it possible for others to replicate the model with the same dataset, or provide access to the model. In general. releasing code and data is often one good way to accomplish this, but reproducibility can also be provided via detailed instructions for how to replicate the results, access to a hosted model (e.g., in the case of a large language model), releasing of a model checkpoint, or other means that are appropriate to the research performed.
- While NeurIPS does not require releasing code, the conference does require all submissions to provide some reasonable avenue for reproducibility, which may depend on the nature of the contribution. For example
  (a) If the contribution is primarily a new algorithm, the paper should make it clear how to reproduce that algorithm.
  (b) If the contribution is primarily a new model architecture, the paper should describe the architecture clearly and fully.
  (c) If the contribution is a new model (e.g., a large language model), then there should either be a way to access this model for reproducing the results or a way to reproduce the model (e.g., with an open-source dataset or instructions for how to construct the dataset).
  (d) We recognize that reproducibility may be tricky in some cases, in which case authors are welcome to describe the particular way they provide for reproducibility. In the case of closed-source models, it may be that access to the model is limited in some way (e.g., to registered users), but it should be possible for other researchers to have some path to reproducing or verifying the results.

5. **Open access to data and code**

Question: Does the paper provide open access to the data and code, with sufficient instructions to faithfully reproduce the main experimental results, as described in supplemental material?

Answer: [Yes]

Justification: The source code is provided in `https://github.com/jehovahxu/CCF`.

Guidelines:

- The answer NA means that paper does not include experiments requiring code.
- Please see the NeurIPS code and data submission guidelines (`https://nips.cc/public/guides/CodeSubmissionPolicy`) for more details.
- While we encourage the release of code and data, we understand that this might not be possible, so "No" is an acceptable answer. Papers cannot be rejected simply for not including code, unless this is central to the contribution (e.g., for a new open-source benchmark).
- The instructions should contain the exact command and environment needed to run to reproduce the results. See the NeurIPS code and data submission guidelines (`https://nips.cc/public/guides/CodeSubmissionPolicy`) for more details.
- The authors should provide instructions on data access and preparation, including how to access the raw data, preprocessed data, intermediate data, and generated data, etc.
- The authors should provide scripts to reproduce all experimental results for the new proposed method and baselines. If only a subset of experiments are reproducible, they should state which ones are omitted from the script and why.
- At submission time, to preserve anonymity, the authors should release anonymized versions (if applicable).
- Providing as much information as possible in supplemental material (appended to the paper) is recommended, but including URLs to data and code is permitted.

6. **Experimental Setting/Details**

Question: Does the paper specify all the training and test details (e.g., data splits, hyperparameters, how they were chosen, type of optimizer, etc.) necessary to understand the results?

Answer: [Yes]

Justification: We provide all the implementation details in Sec. 5 and App. A.

Guidelines:

- The answer NA means that the paper does not include experiments.
- The experimental setting should be presented in the core of the paper to a level of detail that is necessary to appreciate the results and make sense of them.
- The full details can be provided either with the code, in appendix, or as supplemental material.

7. **Experiment Statistical Significance**

Question: Does the paper report error bars suitably and correctly defined or other appropriate information about the statistical significance of the experiments?

Answer: [No]

Justification: All the experiments and comparisons are performed with the same settings.

Guidelines:

- The answer NA means that the paper does not include experiments.
- The authors should answer "Yes" if the results are accompanied by error bars, confidence intervals, or statistical significance tests, at least for the experiments that support the main claims of the paper.
- The factors of variability that the error bars are capturing should be clearly stated (for example, train/test split, initialization, random drawing of some parameter, or overall run with given experimental conditions).
- The method for calculating the error bars should be explained (closed form formula, call to a library function, bootstrap, etc.)
- The assumptions made should be given (e.g., Normally distributed errors).
- It should be clear whether the error bar is the standard deviation or the standard error of the mean.

- It is OK to report 1-sigma error bars, but one should state it. The authors should preferably report a 2-sigma error bar than state that they have a 96% CI, if the hypothesis of Normality of errors is not verified.
- For asymmetric distributions, the authors should be careful not to show in tables or figures symmetric error bars that would yield results that are out of range (e.g. negative error rates).
- If error bars are reported in tables or plots, The authors should explain in the text how they were calculated and reference the corresponding figures or tables in the text.

8. **Experiments Compute Resources**

   Question: For each experiment, does the paper provide sufficient information on the computer resources (type of compute workers, memory, time of execution) needed to reproduce the experiments?

   Answer: [Yes]

   Justification: We provide that in Sec. 5 and App. E.

   Guidelines:

   - The answer NA means that the paper does not include experiments.
   - The paper should indicate the type of compute workers CPU or GPU, internal cluster, or cloud provider, including relevant memory and storage.
   - The paper should provide the amount of compute required for each of the individual experimental runs as well as estimate the total compute.
   - The paper should disclose whether the full research project required more compute than the experiments reported in the paper (e.g., preliminary or failed experiments that didn't make it into the paper).

9. **Code Of Ethics**

   Question: Does the research conducted in the paper conform, in every respect, with the NeurIPS Code of Ethics https://neurips.cc/public/EthicsGuidelines?

   Answer: [Yes]

   Justification: Our research conducted in the paper conforms, in every respect, with the NeurIPS Code of Ethics.

   Guidelines:

   - The answer NA means that the authors have not reviewed the NeurIPS Code of Ethics.
   - If the authors answer No, they should explain the special circumstances that require a deviation from the Code of Ethics.
   - The authors should make sure to preserve anonymity (e.g., if there is a special consideration due to laws or regulations in their jurisdiction).

10. **Broader Impacts**

    Question: Does the paper discuss both potential positive societal impacts and negative societal impacts of the work performed?

    Answer: [Yes]

    Justification: We provide that in App. I.

    Guidelines:

    - The answer NA means that there is no societal impact of the work performed.
    - If the authors answer NA or No, they should explain why their work has no societal impact or why the paper does not address societal impact.
    - Examples of negative societal impacts include potential malicious or unintended uses (e.g., disinformation, generating fake profiles, surveillance), fairness considerations (e.g., deployment of technologies that could make decisions that unfairly impact specific groups), privacy considerations, and security considerations.

- The conference expects that many papers will be foundational research and not tied to particular applications, let alone deployments. However, if there is a direct path to any negative applications, the authors should point it out. For example, it is legitimate to point out that an improvement in the quality of generative models could be used to generate deepfakes for disinformation. On the other hand, it is not needed to point out that a generic algorithm for optimizing neural networks could enable people to train models that generate Deepfakes faster.
- The authors should consider possible harms that could arise when the technology is being used as intended and functioning correctly, harms that could arise when the technology is being used as intended but gives incorrect results, and harms following from (intentional or unintentional) misuse of the technology.
- If there are negative societal impacts, the authors could also discuss possible mitigation strategies (e.g., gated release of models, providing defenses in addition to attacks, mechanisms for monitoring misuse, mechanisms to monitor how a system learns from feedback over time, improving the efficiency and accessibility of ML).

11. **Safeguards**

Question: Does the paper describe safeguards that have been put in place for responsible release of data or models that have a high risk for misuse (e.g., pretrained language models, image generators, or scraped datasets)?

Answer: [NA]

Justification: All the generated images are carefully checked.

Guidelines:

- The answer NA means that the paper poses no such risks.
- Released models that have a high risk for misuse or dual-use should be released with necessary safeguards to allow for controlled use of the model, for example by requiring that users adhere to usage guidelines or restrictions to access the model or implementing safety filters.
- Datasets that have been scraped from the Internet could pose safety risks. The authors should describe how they avoided releasing unsafe images.
- We recognize that providing effective safeguards is challenging, and many papers do not require this, but we encourage authors to take this into account and make a best faith effort.

12. **Licenses for existing assets**

Question: Are the creators or original owners of assets (e.g., code, data, models), used in the paper, properly credited and are the license and terms of use explicitly mentioned and properly respected?

Answer: [Yes]

Justification: We have checked the related requirements.

Guidelines:

- The answer NA means that the paper does not use existing assets.
- The authors should cite the original paper that produced the code package or dataset.
- The authors should state which version of the asset is used and, if possible, include a URL.
- The name of the license (e.g., CC-BY 4.0) should be included for each asset.
- For scraped data from a particular source (e.g., website), the copyright and terms of service of that source should be provided.
- If assets are released, the license, copyright information, and terms of use in the package should be provided. For popular datasets, `paperswithcode.com/datasets` has curated licenses for some datasets. Their licensing guide can help determine the license of a dataset.
- For existing datasets that are re-packaged, both the original license and the license of the derived asset (if it has changed) should be provided.

- If this information is not available online, the authors are encouraged to reach out to the asset's creators.

13. **New Assets**

    Question: Are new assets introduced in the paper well documented and is the documentation provided alongside the assets?

    Answer: [NA]

    Justification: No new assets are provided.

    Guidelines:

    - The answer NA means that the paper does not release new assets.
    - Researchers should communicate the details of the dataset/code/model as part of their submissions via structured templates. This includes details about training, license, limitations, etc.
    - The paper should discuss whether and how consent was obtained from people whose asset is used.
    - At submission time, remember to anonymize your assets (if applicable). You can either create an anonymized URL or include an anonymized zip file.

14. **Crowdsourcing and Research with Human Subjects**

    Question: For crowdsourcing experiments and research with human subjects, does the paper include the full text of instructions given to participants and screenshots, if applicable, as well as details about compensation (if any)?

    Answer: [NA]

    Justification: This paper does not study human subjects.

    Guidelines:

    - The answer NA means that the paper does not involve crowdsourcing nor research with human subjects.
    - Including this information in the supplemental material is fine, but if the main contribution of the paper involves human subjects, then as much detail as possible should be included in the main paper.
    - According to the NeurIPS Code of Ethics, workers involved in data collection, curation, or other labor should be paid at least the minimum wage in the country of the data collector.

15. **Institutional Review Board (IRB) Approvals or Equivalent for Research with Human Subjects**

    Question: Does the paper describe potential risks incurred by study participants, whether such risks were disclosed to the subjects, and whether Institutional Review Board (IRB) approvals (or an equivalent approval/review based on the requirements of your country or institution) were obtained?

    Answer: [NA]

    Justification: This paper does not conduct experiments with human participants.

    Guidelines:

    - The answer NA means that the paper does not involve crowdsourcing nor research with human subjects.
    - Depending on the country in which research is conducted, IRB approval (or equivalent) may be required for any human subjects research. If you obtained IRB approval, you should clearly state this in the paper.
    - We recognize that the procedures for this may vary significantly between institutions and locations, and we expect authors to adhere to the NeurIPS Code of Ethics and the guidelines for their institution.
    - For initial submissions, do not include any information that would break anonymity (if applicable), such as the institution conducting the review.